

가 , CT
 : 가 26 17 G, 1 cm
 가
 2
 24 , 2 , 3 , 1 , 2 , 3 , 4 , 5 , 6
 7 CT (10), {1
 (3), 2 (3), 3 (1): 8 } , {1 (4), 2 (2), 4 (1
), 7 (1): 8 } CT

CT 가
 가 CT
 가 , CT
 가 ,
 가
 CT
 가 (r=0.884, p >0.05).

CT
 CT가

가
 (1, 2),
 (3), (4), 가 , 가
 가 가 (17).

24 Fr

(6, 7). 가 CT
 CT가) 25 mg/kg
 (grounding pad)

가 가 1 cm
 (pulsed technique) 50 W 2

CT , CT

CT

CT

CT

(10)

CT

1 (3), 2 (3), 3 (2)

CT

1 (4), 2 (2), 4 (1),

7 (1)

1

CT

2.5-3 kg New Zealand white rabbit

CT Somatom plus 4 (Siemens,
 Erlangen, Germany) 3 mm ,

CT 가 26

1.6 pitch

1 { : CT

8-9 mL (Ultravist(r), Schering,

(n=3), 3 (n=1)

CT

Berlin, Germany)

} 8 3 { ; 1

2 cc

CT 1 (n=4), 2 (n=2), 4 (n=1), 7

, 30

CT

60

2% lidocaine HCl (Lidocaine : ,

200 W ,) 5 mL

2000 mA

500 KHz

3 mm CT

(CC-1: Radionics, Burlington, MA)

, , 17

G 1 cm 가 (Cool-

, 3

tip single RF electrode)

10%

가

hematoxyline - eosin

가 가

(Watson Marlow Wilmington,

60

CT

Mass)

0 °C

10 - 25 mL/min

CT

Pearson's

(In Vivo Experiments)

s t

Ketamine(50 mg/kg), Xylazine(5 mg/kg)

Student'

10 mg 가

Ketamine 2

cephazolin (CEPHAMEZIN Inj. :

CT

50 W 2
110 - 180 ohm(130 ohm)
10 10 - 15 ohm
40 - 60

가
가

CT

(Fig.

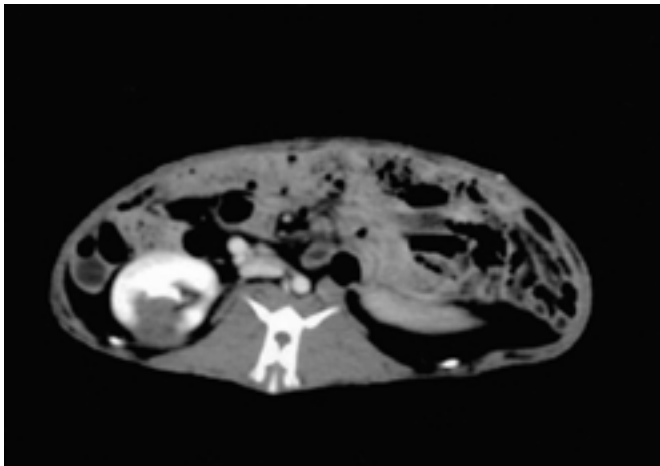
1A).

가
가 (Fig. 3A).

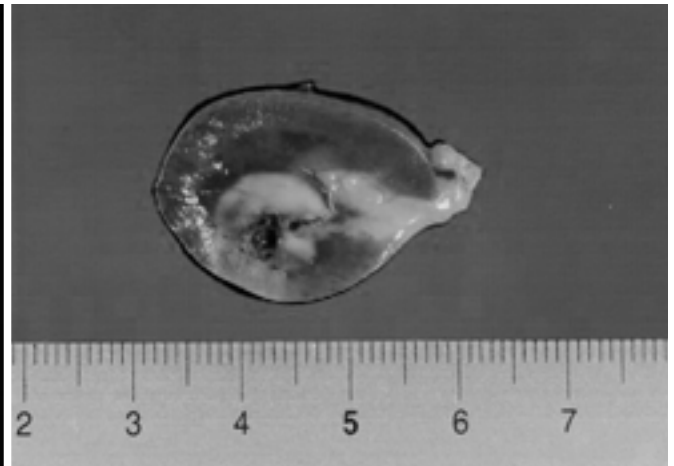
가
(Fig. 1B, 2B).

3

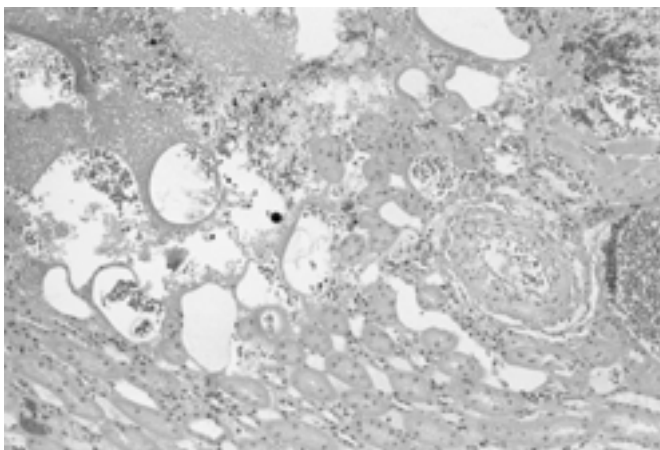
CT



A



B



C

Fig. 1. Acute model: correlation of CT and pathologic findings immediately after RF thermal ablation.

A. Contrast-enhanced CT scan immediately after ablation shows a round area of low attenuation without any evidence of enhancement

B. Gross renal section at the same level as CT scans reveals the ablated lesion that is consisted of a central cavity of tissue loss, a wider zone of pale discolored region, and a peripheral hemorrhagic rim.

C. Histopathologic view (H&E stain, original magnification $\times 100$) shows a interface of the RFA lesion (upper left) and adjacent, uninvolved parenchyma (lower right). Note that the RFA lesion is consisted of a blurring of the nuclear chromatin, an increased eosinophilia of the cytoplasm, loss of cell border integrity, and a presence of interstitial hemorrhage.

(Fig. 3B).

가

CT

± 3.52 mm

(Fig. 3).

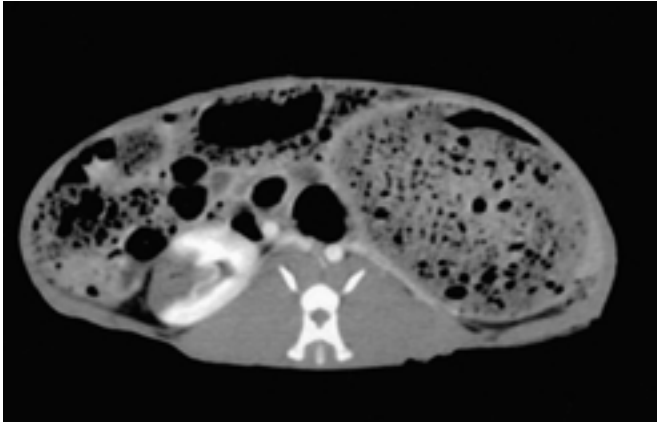
CT

, CT

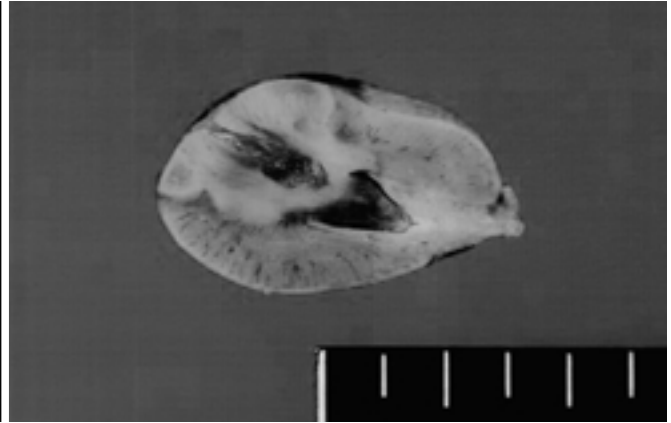
11 - 25 mm

, 17.74

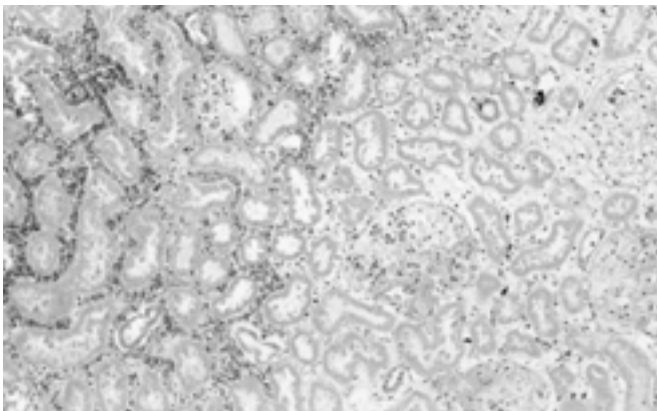
11 - 25 mm,



A



B



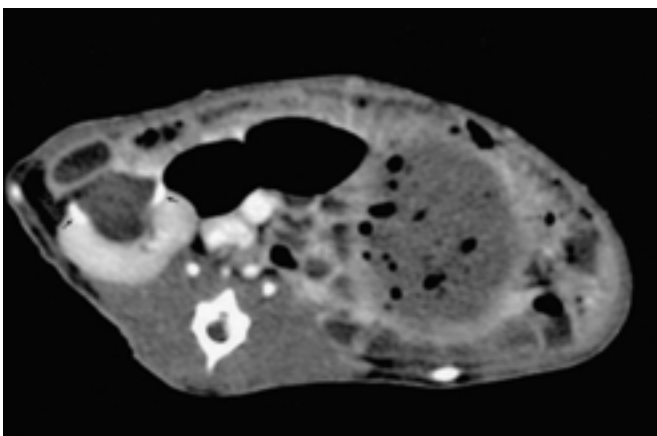
C

Fig. 2. Subacute model: CT images and histologic examination of thermal ablated lesion in rabbit kidney on day 3.

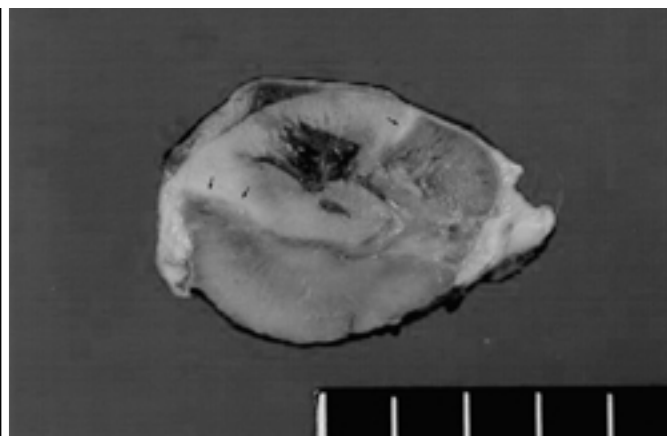
A. Contrast-enhanced axial CT scan shows a wedge shaped perfusion defect with small low attenuated air bubbles.

B. Macroscopic pathologic specimen 3 days after the RF procedure reveals a same configuration of the ablated lesion like CT appearance.

C. Histopathologic view (H & E stain, original magnification $\times 100$) confirms that the ablated lesion has undergone extensive coagulation necrosis. Most of the nuclei had lysed, with few remaining appearing pyknotic.



A



B

Fig. 3. Chronic model: correlation of CT and pathologic findings 2 weeks after RF ablation.

A. Contrast-enhanced axial CT scan through the lesion shows a sharply demarcated, low attenuated zone with peripheral calcifications (arrows) and diminished peripheral rim enhancement compared to acute and subacute model.

B. Macroscopic photograph of the specimen shows a well-demarcated necrotic zone with peripheral calcifications (arrow). Note diminished peripheral hemorrhagic congestion.

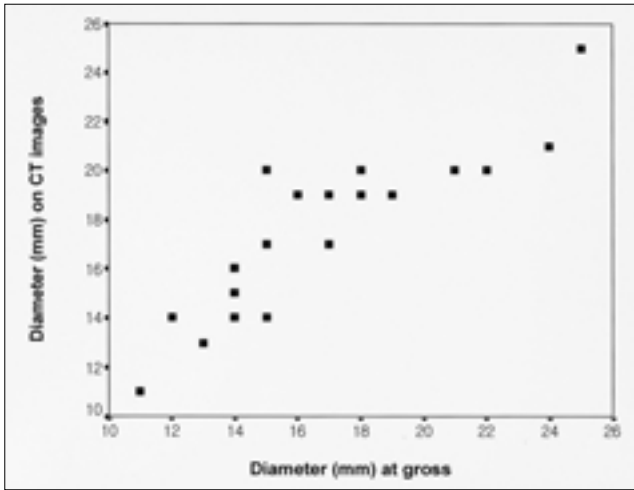


Fig. 4. Radiologic and pathologic correlation curve of maximal diameter of RFA lesions.

16.09 ± 4.02 mm

Pearson 0.884

(Fig. 4).

가 (5).

(5).

50 W, 500 mA

1

2

3

가

(7, 11).

가

가 가

(12, 13).

3

가

가

가 (6, 7).

가

CT

CT가

3 mm

CT

가

CT

CT

CT

가

CT가

가

CT

1. Delworth MG, Pisters LL, Fornage BD, et al. Cryotherapy for renal cell carcinoma and angiomyolipoma. *J Urol* 1996;155:252-255
2. Uchida M, Imaide Y, Sugimoto K, et al. Percutaneous cryosurgery for renal tumors. *Br J Urol* 1995;75:132-137
3. Kagebayashi Y, Hirao Y, Samma S, et al. In situ non-ischemic enu-

cleation of multilocular cystic renal cell carcinoma using a microwave coagulator. *Int J Urol* 1995;2:339-343

4. Susani M, Madersbacher S, Kratzik C, et al. Morphology of tissue destruction induced by focused ultrasound. *Eur Urol* 1993;23:34
5. Gazelle GS, Goldberg SN, Solbiati L, Livraghi T. Tumor ablation with radio-frequency energy. *Radiology* 2000;217:633-646
6. Pater VR, Leveillee RJ, Hoey MF, Herron AJ, Julie Zaias, Hulbert JC. Radiofrequency ablation of rabbit kidney using liquid electrode: acute and chronic observations. *J Endourol* 2000;14:155-159
7. Zlotta AR, Thierry Wildschutz, Gil Raviv, Peny MO, Daniel van Gansbeke, Noel JC, Schulman CC. Radiofrequency interstitial tumor ablation is a possible new modality for treatment of renal cancer: Ex vivo and in vivo experience. *J Endourol* 1997; 11:251-258
8. Metthewson K, Coleridge-Smith P, O SullivnJ, Northfield T, Brown S. Biological effects of intrahepatic neodymium: Yttrium aluminum-garnet laser photocoagulation in rats. *Gastroenterology* 1987;93:550-557
9. Roberts D, Coughlin C, Wong T, Fratkin J, Douple E, Strohhahn J. Interstitial hyperthermia and iridium brachytherapy in treatment of malignant glioma: A phase I clinical trial. *J Neurosurg* 1986;64: 581-587
10. Rossi S, Fornari F, Paties C, Buscarini L. Thermal lesions induced by 480-KHz localized current field in guinea pig and in pig livers. *Tumori* 1990;76:54-57
11. Superstein A, Rogers SJ, Hansen PD, et al. Laparoscopic thermal ablation of hepatic neuroendocrine tumor metastases. *Surgery* 1997;122:1147-1155
12. Polascik TJ, Hamper U, Lee BR, et al. Ablation of renal tumors in a rabbit model with interstitial saline-augmented radiofrequency energy: Preliminary report of a new technology. *Urology* 1998;53: 465-472
13. Thomas HS HSU, Fidler ME, and Gill IS. Radiofrequency ablation of the kidney: Acute and chronic histology in porcine model. *Urology* 2000;56:872-875

Ultrasound-Guided Radiofrequency Thermal Ablation of Normal Kidney in a Rabbit Model: Correlation with CT and Histopathology¹

Sang-Won Kim, M.D., Jeong Min Lee, M.D., Chong Soo Kim, M.D., Sang Hun Lee, M.D.

¹Department of Radiology, Chonbuk National University Hospital

Purpose: To assess the feasibility and safety of using a cooled-tip electrode to perform percutaneous radiofrequency ablation of kidney tissue in rabbits, and to evaluate the ability of CT to reveal the appearance and extent of tissue necrosis during follow-up after ablation.

Materials and Methods: Using ultrasound guidance, a 17-G, cooled-tip electrode was inserted into the right lower portion of the kidney in 26 New Zealand White rabbits. Radiofrequency was applied for 2 mins, and biphasic helical CT scanning was used to assess tissue destruction and the presence or absence of complications immediately after the procedure and at 24 hrs, 2 and 3 days, and 1, 2, 3, 4, 5, 6 and 7 weeks. The study had three phases: acute [immediately killed : N=10]; subacute [killed at 24 hrs (n=3), 2 days (n=3), 3 days (n=1) : N=7]; chronic [killed at 1 week (n=4), 2 weeks (n=2), 4 weeks (n=1), 7 weeks (n=1) : N=8]. After the animals were killed, their kidneys were histopathologically examined and the radiologic and pathologic findings of lesion size and configuration were correlated.

Results: In each instance, ultrasound-guided radiofrequency ablations of the lower pole of the kidney were technically successful. Contrast-enhanced biphasic helical CT revealed regions of hypoattenuation devoid of parenchymal enhancement, and these correlated closely with true pathologic lesion size ($r=0.884$; $p>0.05$). In subacute and chronic models, CT scanning revealed gradual spontaneous resorption of the ablated lesion and the presence of perilesional calcification. Histopathologically, in the acute phase the ablated lesions showed coagulative necrosis and infiltration of inflammatory cells, and in the chronic phase there was clear cut necrosis of glomeruli, tubules and renal interstitium, with diminishing inflammatory response and peripheral fibrotic tissue formation.

Conclusion: Ultrasound-guided renal radiofrequency ablation is technically feasible and safe. In addition, the avascular lesion measured at contrast-enhanced helical CT closely correlated with the size of ablated tissue. Contrast-enhanced CT may therefore be used for serially monitoring the effect of radiofrequency ablation. In the future, RF ablation may offer an alternative treatment option for renal cancer.

Index words : Kidney, interventional procedure
Radiofrequency (RF) ablation

Address reprint requests to : Jeong-Min Lee, M.D., Department of Diagnostic Radiology, Chonbuk National University Hospital,
634-18 Keumam-Dong, Chonju-shi, Chonbuk 561-712, South Korea.
Tel. 82-63-250-1176 Fax. 82-63-272-0481